

RSC Advances



This is an *Accepted Manuscript*, which has been through the Royal Society of Chemistry peer review process and has been accepted for publication.

Accepted Manuscripts are published online shortly after acceptance, before technical editing, formatting and proof reading. Using this free service, authors can make their results available to the community, in citable form, before we publish the edited article. This *Accepted Manuscript* will be replaced by the edited, formatted and paginated article as soon as this is available.

You can find more information about *Accepted Manuscripts* in the [Information for Authors](#).

Please note that technical editing may introduce minor changes to the text and/or graphics, which may alter content. The journal's standard [Terms & Conditions](#) and the [Ethical guidelines](#) still apply. In no event shall the Royal Society of Chemistry be held responsible for any errors or omissions in this *Accepted Manuscript* or any consequences arising from the use of any information it contains.

1 **Pd nanoparticles supported on Mg-Al-CO₃ layered double hydroxide**
2 **as an effective catalyst for methanol electro-oxidation**

3 Zhijun Jia, Yi Wang*, Tao Qi

4 *National Engineering Laboratory for Hydrometallurgical Cleaner Production*
5 *Technology, Institute of Process Engineering, Chinese Academy of Sciences, Beijing*
6 *100190, China*

7 **Corresponding authors: Y. Wang, Fax: (+86) 10 82544848-802, Tel: (+86) 10*
8 *82544967, E-mail: wangyi@ipe.ac.cn*

9
10 **Abstract:** Pd/C and Pd/Mg-Al-CO₃ LDH (Pd/LDH) catalysts were prepared and their
11 catalytic performances for methanol electro-oxidation in the alkaline solution were
12 investigated in this work. The result of cyclic voltammograms proves that Pd/LDH
13 has a much higher specific activity than Pd/C. CO stripping results indicate that
14 Mg-Al-CO₃ LDH could facilitate the oxidative removal of adsorbed CO and improve
15 the CO poison resistance of Pd/LDH catalysts. The chronoamperograms also indicate
16 Pd/LDH has a better stability. All the results imply that Pd/LDH is very promising for
17 probable application in DMFC field. Furthermore, the insight for the increase of the
18 specific activity is discussed in this work.

19 **Keywords:** Palladium nanoparticles; Layered double hydroxide; Electro-catalyst;
20 Methanol electro-oxidation

21

22

1 1. Introduction

2 Direct methanol fuel cells (DMFCs) are attractive as portable power sources
3 primarily owing to their low operating temperature, high energy conversion efficiency,
4 low pollutant emission, low cost and ease of storage [1]. Currently, platinum (Pt) and
5 its alloys are the best electrocatalysts for methanol oxidation but they suffer from high
6 cost, limited reserve and serious poisoning by the strong adsorption of oxidation
7 intermediates, such as CO [2]. Up to date, palladium (Pd), with a similar crystal
8 structure as well as electronic properties as Pt, is a promising alternative to Pt-based
9 electrocatalysts due to its relatively lower cost, good catalytic activity in alkaline
10 media and higher resistance to CO poisoning towards methanol electro-oxidation
11 [2-4]. Although a number of Pd-based catalysts, such as Pd-C and Pd-oxides, have
12 been developed for enhancing the methanol oxidation activity [5-8], it remains
13 challenging to develop excellent catalysts with high electrocatalytic activities which
14 are feasible for practical applications.

15 Layered double hydroxides (LDHs), also known as anionic clays, are a family of
16 layered materials consisting of positively charged brucite-type octahedral layers
17 where the charge-balancing anions and water molecules occupy the interlayer space
18 [9-12]. In recent years, LDHs have attracted growing interest for applications in
19 numerous fields owing to their desirable properties, such as good anion-exchange
20 ability, high thermal stability, and good catalytic activity. For example, Mg-Al-CO₃
21 LDH was manifested as a hydroxide ion conductor due to its anion-exchange ability.
22 An alkaline-type direct ethanol fuel cell (DEFC), using this kind of LDHs as the

1 electrolyte and aqueous solution of ethanol and potassium hydroxide as a source of
2 fuel, exhibits excellent electrochemical performance from room temperature to 80°C:
3 open circuit voltage of 0.87 V and electric power of more than 65 W cm⁻² were
4 obtained [9]. Methanol or ethanol electro-oxidation process is a hydroxide ion related
5 reaction and Mg-Al-CO₃ LDH is a hydroxide ion conductor. Therefore, it will be
6 interesting to see if the incorporation of Pd particles into LDH is a good way to
7 fabricate a new effective catalyst for DMFCs.

8 Herein, we utilized the hydroxide conductor (Mg-Al-CO₃ LDH) and carbon black
9 (XC-72, Gashub), as support materials, synthesized Pd/Mg-Al-CO₃ LDH and Pd/C
10 catalysts and investigated the electrocatalytic activity of the as-prepared catalysts for
11 methanol oxidation. Furthermore, the insight for the increase of the specific activity
12 was also discussed in this work.

13

14 **2. Experimental**

15 2.1 Preparation of Mg-Al-CO₃ LDH

16 In a typical synthesis, co-precipitated Mg-Al-CO₃ LDH was synthesized by
17 simultaneous dropwise addition of 30 mL of 1.0 M Mg(NO₃)₂ and 30 mL of 0.5 M
18 Al(NO₃)₃ solutions to 100 mL of 1.5 M Na₂CO₃ solution during constant stirring. The
19 pH was adjusted to ~10 by addition of NaOH solution. Then the vessel was
20 transferred to water bath kept at 65°C for 6 hours. Finally the precipitate was filtered,
21 washed with deionized water, and dried in air at 80°C.

22 2.2 Preparation of catalysts

1 To synthesize the electrocatalysts, 100 mg support materials including carbon black
2 and Mg-Al-CO₃ LDH were added into 75 mL deionized water and ultra-sonicated for
3 8 min, respectively. Then 41.7 mg PdCl₂ and 103.7 mg sodium citrate
4 (Na₃C₆H₅O₇·2H₂O) were added into above suspensions. Afterwards, excess amount of
5 0.01 M NaBH₄ aqueous solution (freshly prepared) was added dropwise, followed by
6 stirring for 6 hours at room temperature. Finally, the suspensions were filtered and
7 washed several times with deionized water, and the remaining solids were dried at 60°C
8 overnight. The catalysts were harvested and denoted as Pd/C and Pd/LDH,
9 respectively. The theoretical content of Pd is 20 wt%.

10 2.3 Characterization of catalysts

11 Structure and morphology of the catalysts were investigated by X-ray diffraction
12 (XRD, Smartlab (9 kw), Cu K α) and transmission electron microscopy (TEM,
13 JEM-2100, 200 kV). The elemental analysis was performed by Inductively Coupled
14 Plasma Atomic Emission Spectrometry (ICP-AES, IRIS Intrepid II XSP
15 (ThermoFisher)). The nature of surface species of catalysts was investigated by X-ray
16 photoelectron spectroscopy (XPS, Escalab 250Xi).

17 The electrochemical measurements were conducted on an electrochemical
18 workstation system (CHI760D, Chenhua, Shanghai, China) with a three-electrode cell
19 using Pt foil and HgO/Hg electrode as the counter and reference electrodes,
20 respectively. The working electrode was prepared by dropping 5 μ L of the
21 electrocatalyst ink onto glassy carbon electrode (GCE). The ink was prepared by
22 ultrasonically mixing 5 mg electrocatalyst sample in 2 mL of ethanol for 8 min. Then

1 2 μ L of Nafion solution was dropped on top to fix the electrocatalysts. All potentials in
2 this work were given versus HgO/Hg electrode. Cyclic voltammetry (CV) was
3 performed in a 1.0 M KOH+1.0 M methanol solution, where oxygen was removed by
4 purging N₂ for 15 min. The CV experiments were conducted at a sweep rate of 50 mV
5 s⁻¹, with potentials ranging from -0.8 V to 0.3 V. Electrochemical impedance
6 spectrums (EIS) were measured at -0.2 V from 100 KHz to 0.01 Hz and the perturbing
7 AC amplitude was 5 mV. CO stripping experiments were performed as follows: after
8 purging the solution with N₂ for 20 min, gaseous CO was bubbled for 15 min to form
9 CO adlayer on catalysts while maintaining potential at -0.8 V. Then excess CO in
10 solution was purged with N₂ for 20 min and CO stripping voltammetry was recorded
11 in 1 M KOH solution at 50 mV s⁻¹. The chronoamperometry (CA) was conducted at
12 -0.15 V for 3600 s.

13

14 **3. Results and discussion**

15 3.1 Structural and compositional analysis

16 XRD patterns of the Pd/C and Pd/LDH catalysts are shown in Fig. 1(a). There are
17 five diffraction peaks corresponding to (111), (200), (220), (311) and (222) planes of
18 Pd at ca. 40.1, 46.6, 68.1, 82.1 and 86.6°, respectively [13-15]. The diffraction peak at
19 ca. 25° in the pattern of Pd/C belongs to the characteristic peak of carbon [15]. For
20 Pd/LDH catalyst, other peaks except that associated with metallic Pd are well
21 matched with the characteristic peaks of Mg-Al-CO₃ LDH [9]. According to
22 Debye-Scherrer equation, the diameters of Pd particles on Pd/C and Pd/LDH are

1 11.54 and 7.89 nm, respectively. Fig. 1 (f) presents the morphology of Mg-Al-CO₃
2 LDH and it is apparent to see the nanosheet structure of this as-prepared sample.
3 Therefore, Mg-Al-CO₃ LDH can be used as a catalyst support material. Fig. 1(b)-(e)
4 show the TEM images and particle size distributions of the as-prepared catalysts. It
5 can be seen that metal nanoparticles are dispersed uniformly on the support materials.
6 The uniform distribution may be attributed to: 1) the support material sheets could
7 provide more locations for the reduction reaction; 2) sodium citrate plays an
8 anti-precipitation effect to manipulate the particle size and 3) sodium citrate also
9 could inhibit the aggregation of the metal particles and make Pd distribute uniformly
10 on the support materials. The average sizes of Pd particles in Pd/C and Pd/LDH
11 catalysts analyzed from TEM images are 8.86 and 5.96 nm, respectively, which are
12 smaller than those obtained from Debye-Scherrer equation. Additionally, according to
13 ICP-AES analysis results, the real mass percentages of Pd in Pd/C and Pd/LDH
14 catalysts are 18.83 and 17.68%, respectively.

15 XPS was further employed to examine the surface electron structure of the
16 as-prepared samples. Pd3d core level spectra of Pd/C and Pd/LDH catalysts were
17 presented in Fig. 2 (a) and (b) and were fitted by two pairs of overlapping Lorentzian
18 curves [14-15]. In Pd3d XPS spectra for Pd/C, the more intense peaks (335.87 and
19 340.2 eV) were assigned to metallic palladium, Pd(0). The other set of doublets
20 (336.7 and 341.9 eV) can be attributed to the Pd(□) chemical state on PdO or
21 Pd(OH)₂. Pd3d XPS spectra on the as-prepared Pd/LDH catalyst, shown in Fig. 2(b),
22 are also constructed by two sets of doublets which are associated with metallic Pd(0)

1 and Pd(\square). However, the relative intensity of metallic Pd(0) in Pd/LDH is 73.38%,
2 higher than 51.24% obtained from Pd/C. Table 1 lists the relative intensity of Pd(0)
3 and Pd(\square) of the as-prepared catalysts. The results indicate that Mg-Al LDH can
4 increase the content of Pd(0) in Pd/LDH catalyst. As shown in Fig. 2 (c) and (d), there
5 is no obvious change of chemical state for Mg and Al in Pd/LDH and Mg-Al LDH.
6 Therefore, it suggests that Mg-Al LDH may act as a catalyst to enhance Pd(\square)
7 reduction process.

8 3.2 Electrochemical properties of Pd/Mg-Al-CO₃ LDH catalyst

9 It is known that the activity of a catalyst is not only controlled by its catalytic
10 properties but also by the geometrical properties, and the electrochemical surface area
11 (*ESA*) of the catalysts can be calculated using Pd oxide reduction voltammetry by
12 following equation:

$$13 \quad ESA = \frac{S_R}{\nu \times Q_{Pd} \times m_c}$$

14 where S_R is the Pd oxide reduction peak area in voltammetry; ν is the scan rate; Q_{Pd} is
15 the charge needed for the reduction of single layer of oxide on Pd, which is 0.000405
16 C cm⁻² and m_c is the loading amount of catalyst.

17 According to the background cyclic voltammograms of Pd/C and Pd/LDH in 1 M
18 KOH solution at a scan rate of 50 mV s⁻¹, shown in Fig. 3(a), ESAs of Pd/C and
19 Pd/LDH were 28.03 and 29.01 m² g⁻¹, respectively. Therefore, there is no apparent
20 difference in *ESAs* of the as-prepared catalysts.

21 The cyclic voltammograms of methanol oxidation on these two catalysts are shown
22 in Fig. 3 (b). The magnitude of the peak current on the forward scanning direction

1 indicates the electrocatalytic activity of the electrocatalyst for methanol oxidation [12].
2 The forward peak current density of the Pd/LDH is higher than that of Pd/C and the
3 result suggests the electrocatalytic activity of Pd/LDH is much higher than that of
4 Pd/C. Furthermore, the higher anodic current on Pd/LDH indicates the presence of
5 LDH can improve the electrocatalytic activity of Pd/LDH for methanol oxidation.

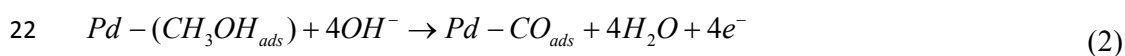
6 EIS was further applied to analyze the electrocatalytic performance of Pd/C and
7 Pd/LDH. Fig. 4 (a) represents the EIS plots of Pd/C and Pd/LDH at -0.2V in 1.0 M
8 KOH+1.0 M methanol solution and the data was analyzed by the electric equivalent
9 circuit shown in Fig. 4(b). In the electric equivalent circuit, R_s is the sum of resistance
10 of electrolyte, electrode material and the contact resistance at the interface of the
11 active material/current collector; C represents the double layer capacitance; R_t is the
12 charge transfer resistance; R_c is the resistance of intermediate adlayer and L is the
13 inductance induced by the intermediate. The values of R_s , C , R_t , R_c and L were
14 calculated from the CNLS fitting of the experimental impedance spectra and their
15 resulting values are listed in Table 2.

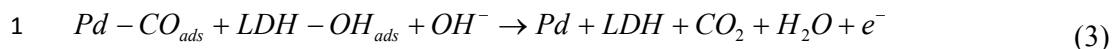
16 According to the fitting results in Table 2, it is apparent to see the resistances for
17 Pd/LDH, no matter R_t or R_c , are smaller than that for Pd/C. Therefore, Pd/LDH shows
18 a better performance in methanol electro-oxidation process than Pd/C. Furthermore,
19 Pd/LDH has smaller double layer capacitance (C) and inductance (L) generated by the
20 intermediate than Pd/C catalyst. It indicates that less amount of intermediate in the
21 methanol electro-oxidation process adsorbed on Pd/LDH surface. Pd/LDH may have
22 a better CO poisoning resistance than Pd/C.

1 To further evaluate the resistance to the CO_{ads} poisoning of each catalyst, the CO
 2 stripping voltammograms were recorded, as shown in Fig. 5. It is clear that the onset
 3 potential of CO oxidation on Pd/LDH catalyst is more negative than that on Pd/C
 4 catalyst, indicating that Mg-Al-CO₃ LDH facilitates the removal of CO out of the
 5 surface of the Pd/LDH catalyst owing to the potential adsorption and conduction of
 6 OH⁻. Furthermore, due to the catalytic effect, Mg-Al-CO₃ LDH could activate water
 7 at lower potentials than Pd. The activated water could oxidize the adsorbed CO and
 8 liberated Pd active sites [15-16]. This result helped to explain the higher activity of
 9 Pd/LDH catalyst for the oxidation of methanol.

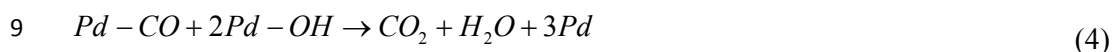
10 The above analytic results confirm that Pd/LDH composite has a better
 11 electrocatalytic activity for methanol oxidation in KOH. The probable reason for this
 12 trend is summarized as follows: 1) content increase of metallic state palladium in the
 13 Pd/LDH catalyst, which is well known that the more content of metallic state in
 14 catalysts, the better catalytic performance; 2) as a hydroxide ion conductor,
 15 Mg-Al-CO₃ LDH could deliver OH⁻ and increase the concentration of OH⁻ around Pd
 16 particle surface, as shown in scheme 1.

17 The better CO poisoning resistance of Pd/LDH also can be explained as follows:
 18 the surface adsorbed hydroxyl of Mg-Al-CO₃ LDH may remove the adsorbed
 19 carbonyl on the surface of Pd, and then dissociation-adsorption of methanol proceeds
 20 quickly. The reaction can be written as Equation. 1~3.





2 Mg-Al-CO₃ LDH would increase the concentration of OH_{ads} species on the catalyst
3 surface, and these OH_{ads} can react with CO-like intermediate species to produce CO₂
4 or water soluble products, releasing the active sites on Pd for further electrochemical
5 reaction [12]. Furthermore, the other reason for CO tolerance improvement is the
6 so-called wetness effect of Mg-Al-CO₃ LDH on the primary Pd-OH oxide spillover,
7 which is considered decisive for CO oxidation [17-18], as shown in the following
8 equation (4).



10 The long-term stability of Pd/C and Pd/LDH catalysts for the oxidation of methanol
11 at a potential of -0.15 V were also investigated and the chronoamperometry curves are
12 shown in Fig.6. Due to the formation of some Pd oxides/hydroxides and adsorbed
13 intermediates in the alcohol electro-oxidation reaction, all these catalysts show a
14 current decay before a steady current status was attained [9, 15]. As expected, the
15 current density of Pd/LDH was larger than that of Pd/C in methanol solution. In
16 addition, in the beginning, the current for Pd/LDH declined more slowly than that for
17 Pd/C. This also proves that Pd/LDH has better electrochemical catalytic stability for
18 the oxidation of methanol than Pd/C.

19

20 4. Conclusions

21 Pd/C and Pd/Mg-Al-CO₃ LDH catalysts were prepared and their catalytic
22 performance for methanol electro-oxidation was compared. Cyclic voltammograms in

1 the alkaline solution showed the much higher specific activity of Pd/LDH than that of
2 Pd/C. The increase of the specific activity could be attributed to the OH⁻ conductivity
3 of Mg-Al-CO₃ LDH and the content increase of metallic Pd. According to CO
4 stripping results, it is found that Mg-Al-CO₃ LDH facilitates the oxidative removal of
5 adsorbed CO. The chronoamperograms indicated that Pd/LDH has a better stability.
6 All the results imply that Pd/LDH is very promising for probable application in
7 DMFC field. Furthermore, Mg-Al-CO₃ LDH may act two important roles in the
8 Pd/LDH catalyst: 1) catalyst for Pd(□) reduction, 2) facilitating hydroxide ion
9 conduction.

10

11 **Acknowledgement**

12 The authors are grateful for the financial support by One Hundred Talent Program
13 of Chinese Academy of Sciences, Chinese National Programs for High Technology
14 Research and Development (2014AA06A513), as well as by the NSFC (51302264) of
15 China.

16

17

18 **References**

- 19 1. W. Li, X.S. Zhao, A. Manthiram, Room-temperature synthesis of Pd/C cathode
20 catalysts with superior performance for direct methanol fuel cells, *J. Mater. Chem.*
21 *A* 2 (2014) 3468-3476.
- 22 2. R. Liu, H.H. Zhou, J. Liu, Y. Yao, Z.Y. Huang, C.P. Fu, Y.F. Kuang, Preparation of

- 1 Pd/MnO₂-reduced graphene oxide nanocomposite for methanol electro-oxidation
2 in alkaline media, *Electrochem. Commun.* 26 (2013) 63-66.
- 3 3. C.X. Xu, Y.Q. Liu, Q. Hao, H.M. Duan, Nanoporous PdNi alloys as highly active
4 and methanol-tolerant electrocatalysts towards oxygen reduction reaction, *J. Mater.*
5 *Chem. A* 1 (2013) 13542-13548.
- 6 4. L.Z. Li, M.X. Chen, G.B. Huang, N. Yang, L. Zhang, H. Wang, Y. Liu, W. Wang,
7 J.P. Gao, A green method to prepare Pd-Ag nanoparticles supported on reduced
8 graphene oxide and their electrochemical catalysis of methanol and ethanol
9 oxidation, *J. Power Sources* 263 (2014) 13-21.
- 10 5. H.R. Zhao, Q.H. Tang, Y. Wang, T. Qi, X. Wang, Pd nanoparticles supported on
11 PDDA-functionalized Ti₄O₇ as an effective catalyst for formic acid
12 electrooxidation, *ECS Solid State Lett.* 3 (2014) M37-M40.
- 13 6. Y.L. Wang, D.D. Zhang, W. Peng, L. Liu, M.G. Li, Electrocatalytic oxidation of
14 methanol at Ni-Al layered double hydroxide film modified electrode in alkaline
15 medium, *Electrochim. Acta* 56 (2011) 5754-5758.
- 16 7. Y.L. Wang, D.D. Zhang, M. Tang, S.D. Xu, M.G. Li, Electrocatalysis of gold
17 nanoparticles/layered double hydroxides nanocomposites toward methanol
18 electro-oxidation in alkaline medium, *Electrochim. Acta* 55 (2010) 4045-4049.
- 19 8. Y.L. Wang, H.Q. Ji, W. Peng, L. Liu, F. Gao, M.G. Li, Gold nanoparticle-coated
20 Ni/Al layered double hydroxides on glassy carbon electrode for enhanced
21 methanol electro-oxidation, *Int. J. Hydrogen Energ.* 37 (2012) 9324-9329.
- 22 9. K. Tdanaga, Y. Furukawa, A. Hayashi, M. Tatsumisago, Direct ethanol fuel cell

- 1 using hydrotalcite clay as a hydroxide ion conductive electrolyte, *Adv. Mater.* 2
2 (2010): 4401-4404.
- 3 10. M.F. Shao, F.Y. Ning, J.W. Zhao, M. Wei, D.G. Evans, X. Duan, Hierarchical
4 layered double hydroxide microspheres with largely enhanced performance for
5 ethanol electrooxidation, *Adv. Funct. Mater.* 23 (2013) 3513-3518.
- 6 11. G. Karim-ezhad, S. Pashazadeh, A. Pashazadeh, Electrocatalytic oxidation of
7 methanol and ethanol by carbon ceramic electrode modified with Ni/Al LDH
8 nanoparticles, *Chin. J. Catal.* 33 (2012)1809-1816.
- 9 12. Y.C. Zhao, L. Zhan, J.N. Tian, S.L. Nie, Z. Ning, MnO₂ modified multi-walled
10 carbon nanotubes supported Pd nanoparticles for methanol electro-oxidation in
11 alkaline media, *Int. J. Hydrogen Energ.* 35 (2010) 10522-10526.
- 12 13. C.W. Xu, H. Wang, P.K. Shen, S.P. Jiang, Highly ordered Pd nanowire arrays as
13 effective electrocatalysts for ethanol oxidation in direct alcohol fuel cells, *Adv.*
14 *Mater.* 19 (2007) 4256-4259.
- 15 14. L. Wang, Y. Wang, A. Li, Y.S. Yang, J. Wang, H.R. Zhao, X. Du, T. Qi,
16 Electrocatalysis of carbon black- or chitosan-functionalized activated carbon
17 nanotubes-supported Pd with a small amount of La₂O₃ towards methanol
18 oxidation in alkaline media, *Int. J. Hydrogen Energ.* 39 (2014) 14730-14738.
- 19 15. L. Wang, Y. Wang, A. Li, Y.S. Yang, Q.B. Tang, H.B. Cao, T. Qi, C.M. Li,
20 Electrocatalysis of carbon black-or poly (diallyldimethyl- ammonium
21 chloride)-functionalized activated carbon nanobutes-supported Pd-Tb towards
22 methanol oxidation in alkaline media, *J. Power Sources* 257 (2014) 138-146.

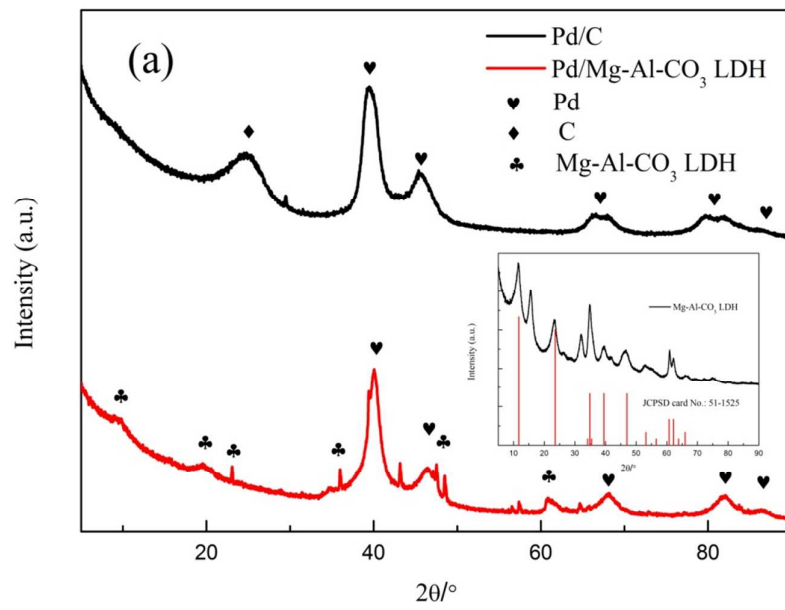
- 1 16. H.R. Zhao, Y. Wang, Q.H. Tang, L. Wang, H. Zhang, C. Quan, T. Qi, Pt catalyst
2 supported on titanium suboxide for formic acid electrooxidation reaction, *Int. J.*
3 *Hydrogen Energ.* 39 (2014) 9621-9627.
- 4 17. J.M. Jaksic, Lj. Vracar, S.G. Neophytides, S. Zafeiratos, G. Papakonstantinou, N.V.
5 Krstajic, M.M. Jaksic, Structural effects on kinetic properties for hydrogen
6 electrode reactions and CO tolerance along Mo-Pt phase diagram, *Surf. Sci.* 598
7 (2005) 156-173.
- 8 18. J.M. Jaksic, C.M. Lacnjevac, N.V. Krstajic, M.M. Jaksic, Interactive supported
9 electrocatalysts and spillover effect in electrocatalysis for hydrogen and oxygen
10 electrode reaction, *Chem. Ind. Chem. Eng. Q.* 14 (2008) 119-136.

11

- 1 Figure caption
- 2 Fig.1 (a) XRD patterns of Pd/C and Pd/LDH (inset: XRD pattern of Mg-Al-CO₃
- 3 LDH); (b) TEM image of Pd/C; (c) Diameter distribution of Pd Particles on Pd/C; (d)
- 4 TEM image of Pd/LDH; (e) Diameter distribution of Pd Particles on Pd/LDH and (f)
- 5 TEM image of Mg-Al-CO₃ LDH
- 6 Fig. 2 (a) XPS spectra of Pd of Pd/C; (b) XPS spectra of Pd of Pd/LDH; (c) XPS
- 7 spectra of Mg of Mg-Al LDH and Pd/LDH; (d) XPS spectra of Al of Mg-Al LDH and
- 8 Pd/LDH
- 9 Fig. 3 The cyclic voltammograms of Pd/C and Pd/LDH in 1.0 M KOH (a) and in 1.0
- 10 M KOH+1.0 M methanol solution (b)
- 11 Fig. 4 EIS plots of Pd/C and Pd/LDH at different potentials (a, b) and equivalent
- 12 electrical circuit in 1.0 M KOH+1.0 M methanol solution
- 13 Fig. 5 CO stripping curves on Pd/C (a) and Pd/LDH (b) catalysts recorded in 1 M
- 14 KOH solution
- 15 Scheme 1 Function of Mg-Al-CO₃ LDH in the methanol electro-oxidation at Pd
- 16 particle surface
- 17 Fig.6 Chronoamperograms of Pd/C and Pd/LDH in 1.0 M KOH+1.0 M methanol at
- 18 operation potential of -0.15 V at 25°C
- 19
- 20
- 21
- 22

1

Fig. 1 (a)

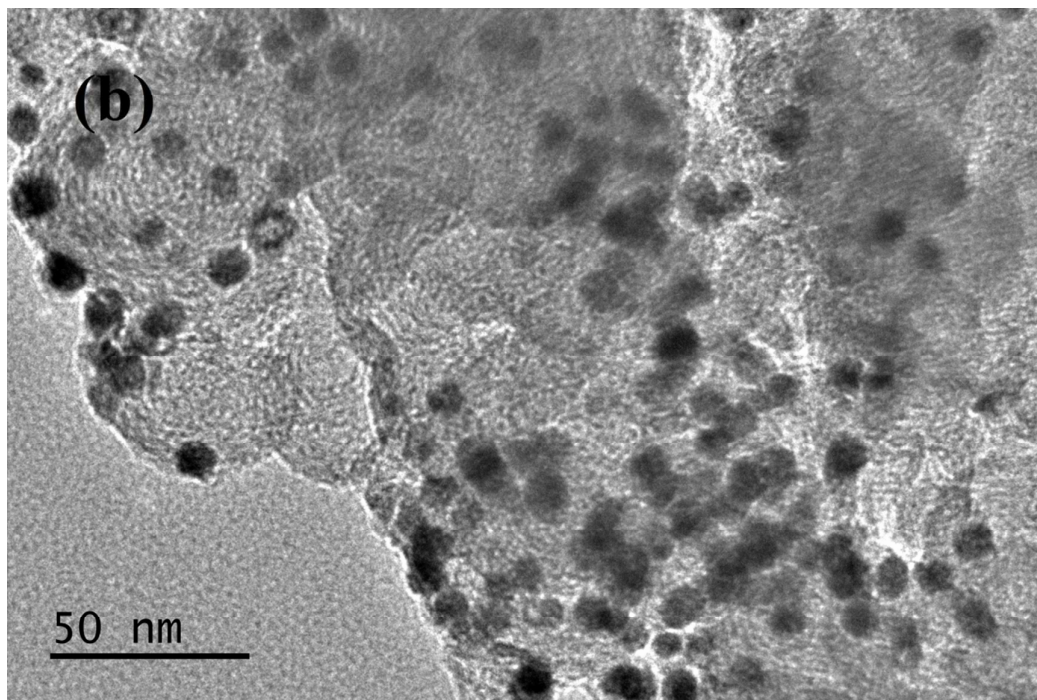


2

3

1

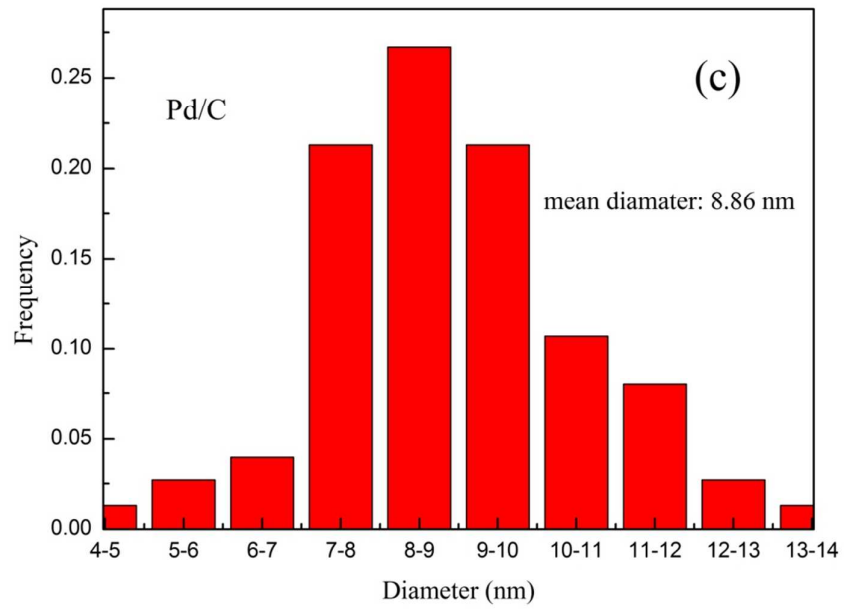
Fig. 1 (b)



2
3

1

Fig. 1(c)

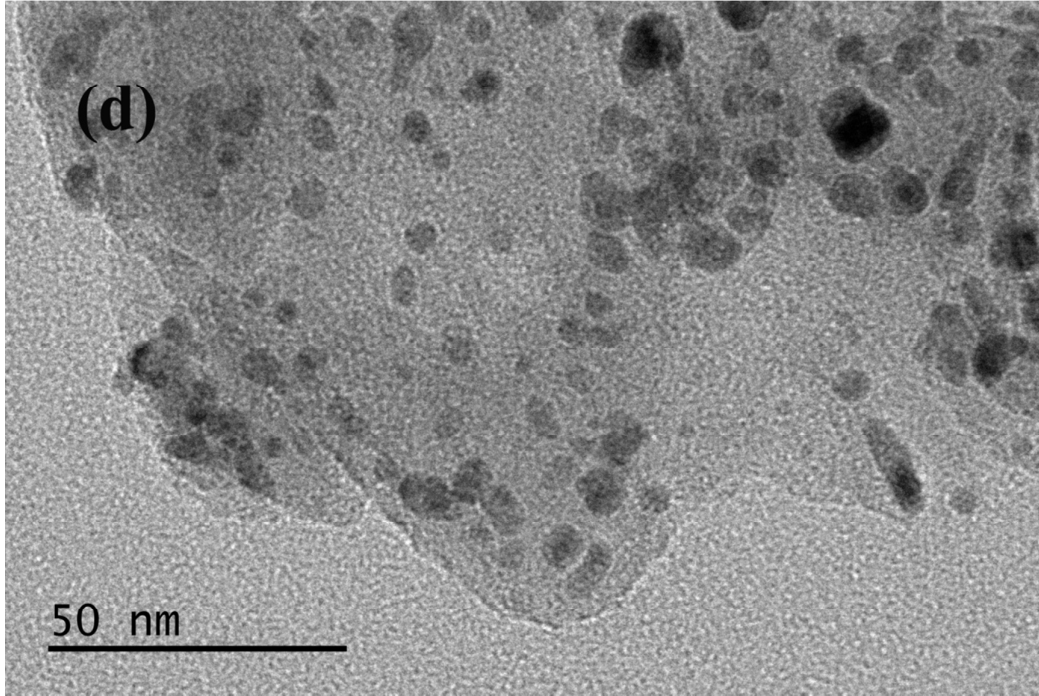


2

3

1

Fig. 1 (d)

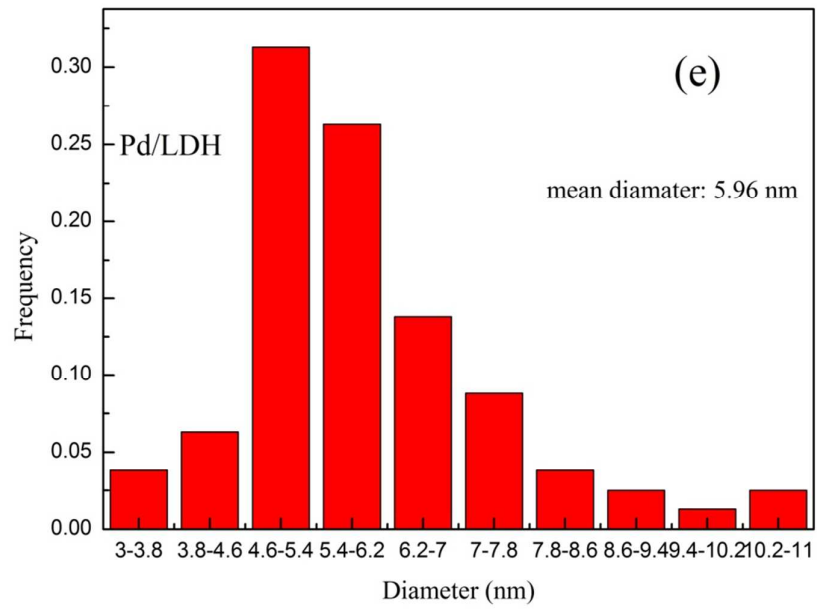


2

3

1

Fig. 1 (e)

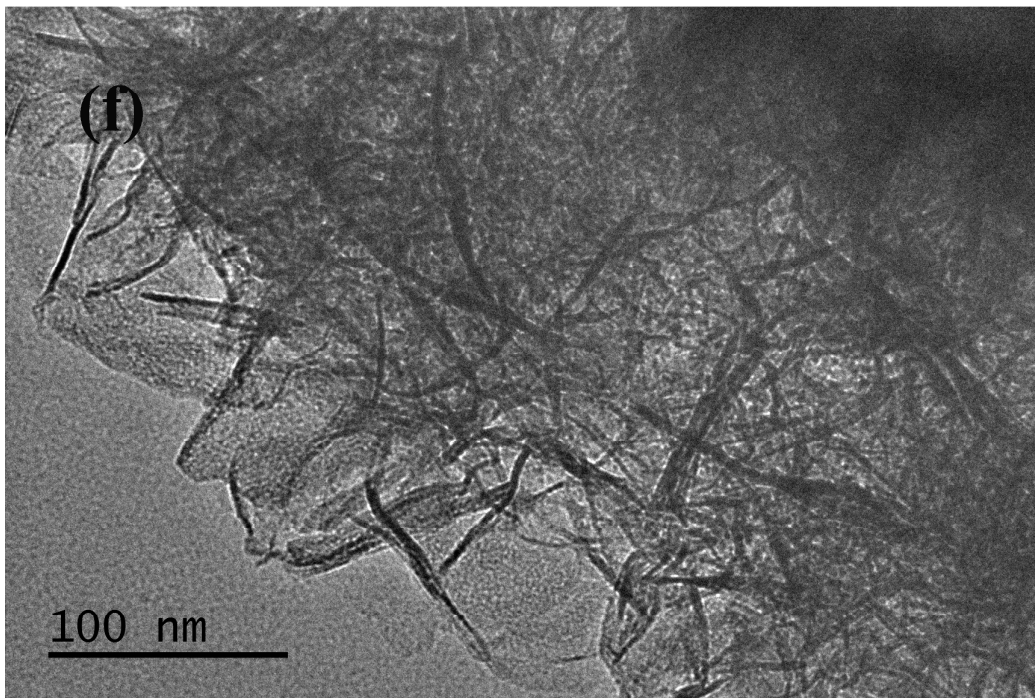


2

3

1

Fig. 1(f)



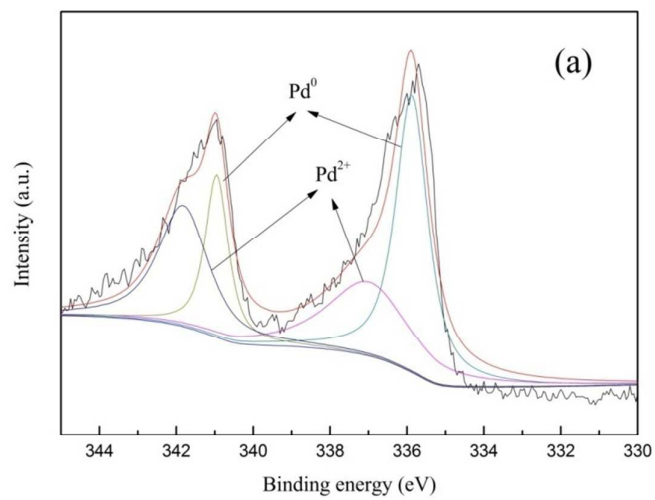
2

3

4

1

Fig. 2 (a)

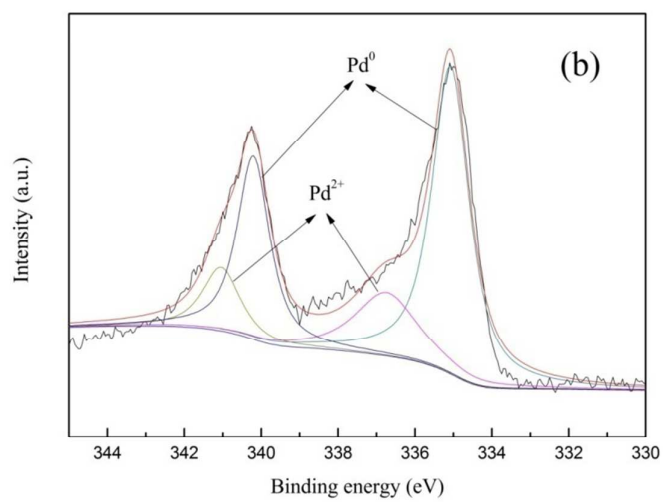


2

3

1

Fig. 2 (b)

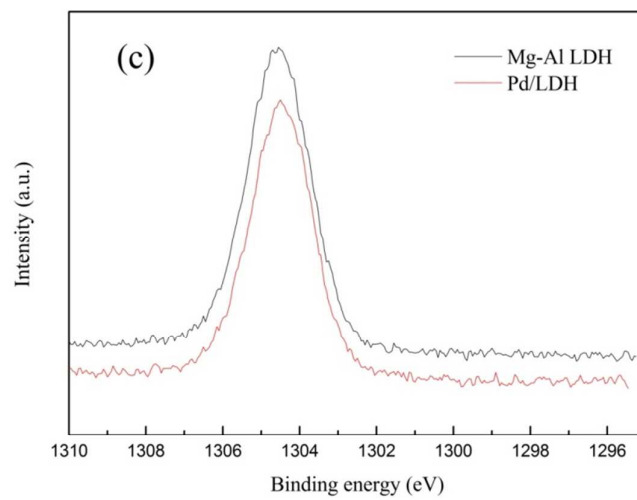


2

3

1

Fig. 2 (c)

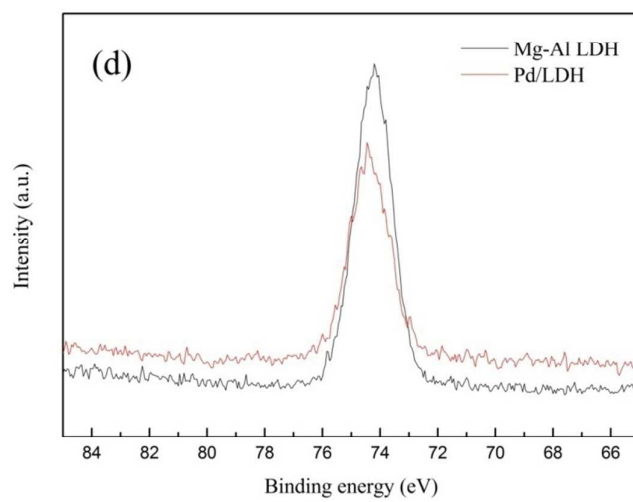


2

3

1

Fig. 2 (d)



2

3

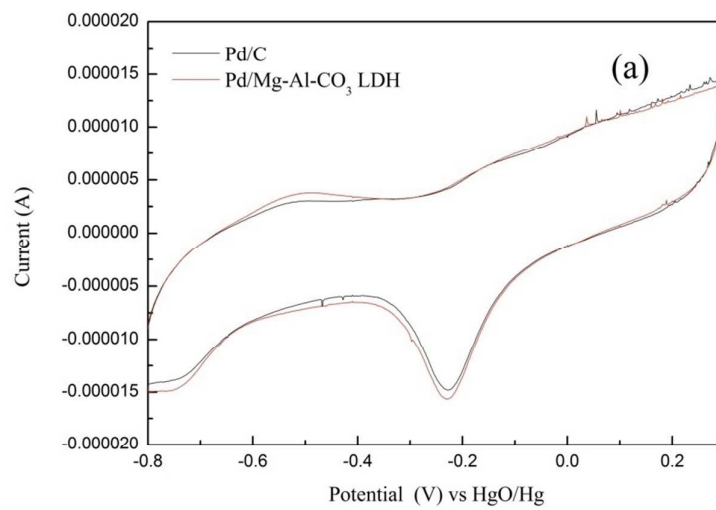
4

5

6

1

Fig. 3 (a)

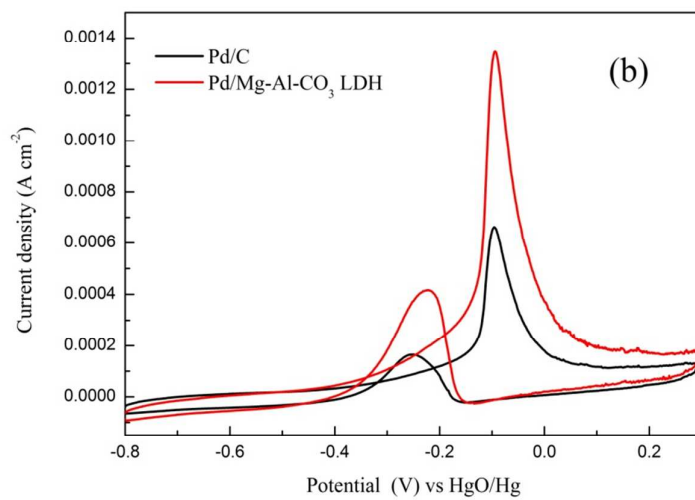


2

3

1

Fig. 3 (b)



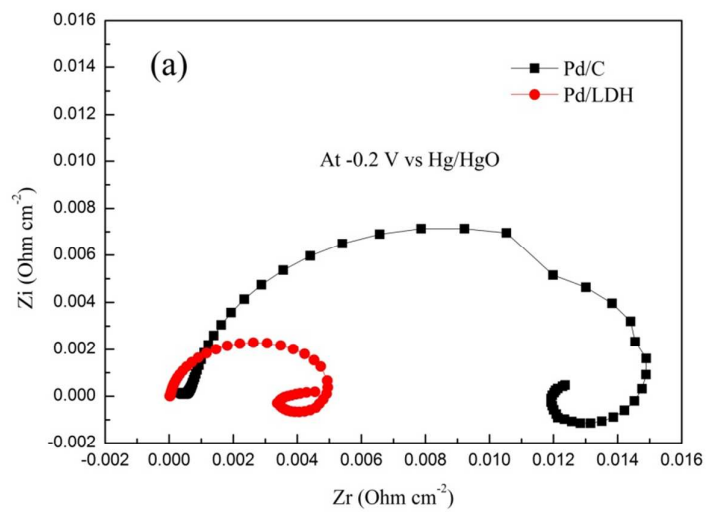
2

3

4

1

Fig. 4 (a)

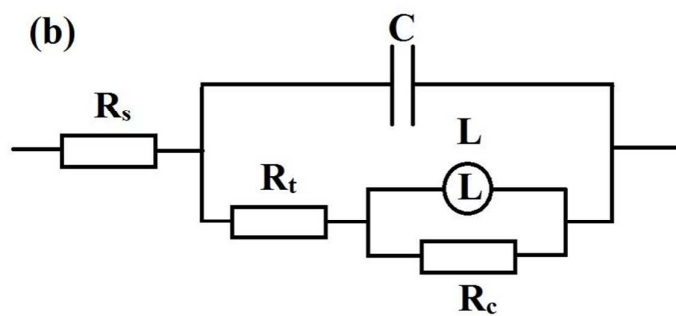


2

3

1

Fig. 4 (b)

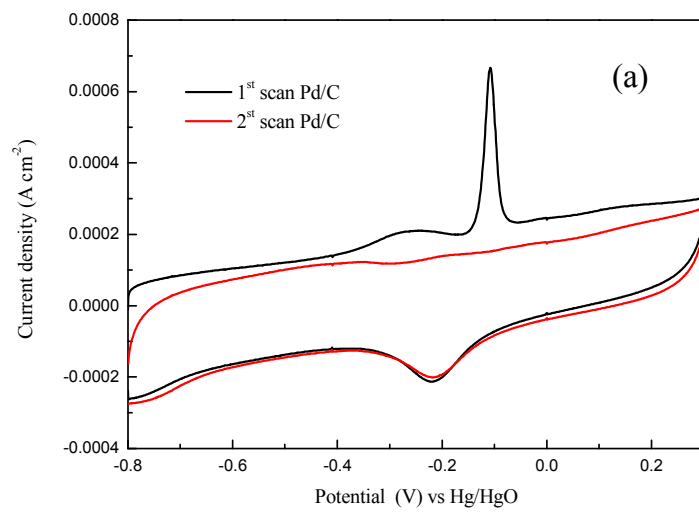


2

3

1

Fig. 5 (a)

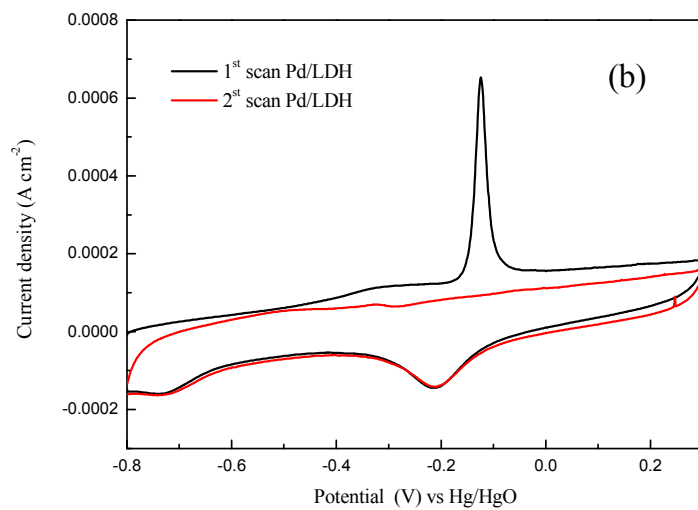


2

3

1

Fig. 5 (b)



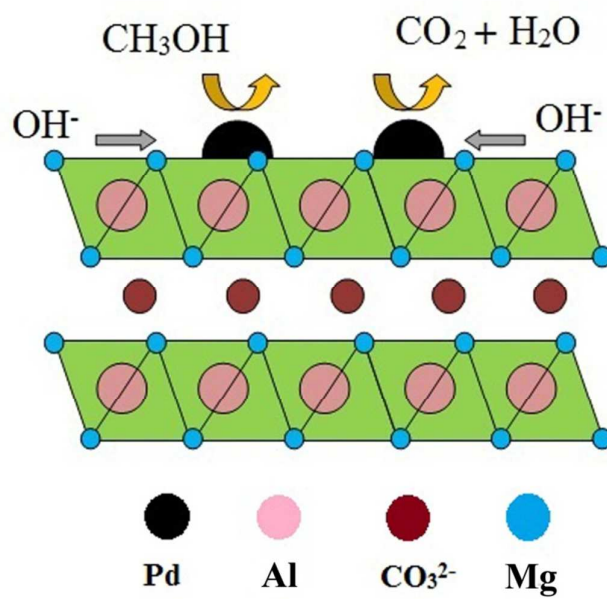
2

3

4

1

Scheme 1



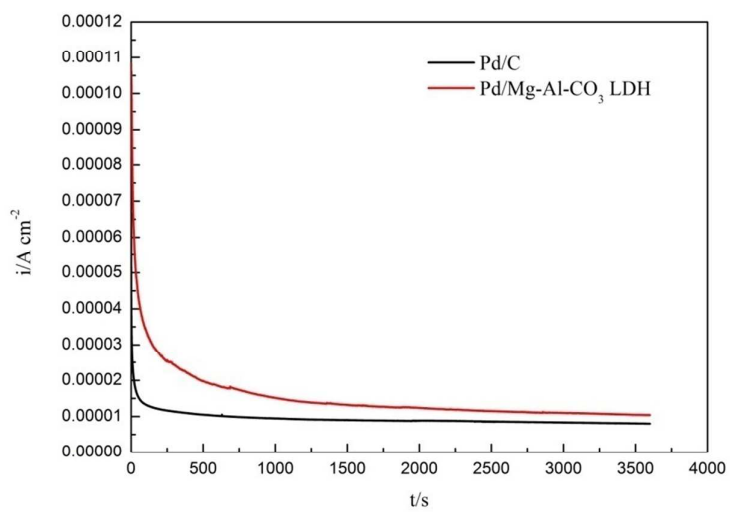
2

3

4

1

Fig.6



2

3

4

5

6

- 1 Table caption
- 2 Table 1 Binding energy (B.E.) and relative intensity of species from curve-fitted XPS
- 3 spectra of Pd3d
- 4 Table 2 Fitting results of EIS (All the fitting data were normalized by *ESA*)
- 5
- 6
- 7
- 8

1

Table 1

Samples	B.E. of Pd 3D _{5/2} (eV)	B.E. of Pd 3D _{3/2} (eV)	Species	Relative intensity (%)
Pd/C	335.87	340.2	Pd(0)	51.24
	336.7	341.9	Pd(□)	48.76
Pd/LDH	335.7	341	Pd(0)	73.38
	336.51	342.1	Pd(□)	26.62

2

3

1

Table 2

	R_s ($\Omega \text{ cm}^2$)	C (F cm^{-2})	R_t ($\Omega \text{ cm}^2$)	R_c ($\Omega \text{ cm}^2$)	L (H cm^{-2})
Pd/C	5.53625E-4	9.48125E-9	0.01139	0.00227	0.00248
Pd/LDH	3.19302E-5	4.8924E-11	0.00364	4.30515E-4	0.00119

2

3